Available online at www.sciencedirect.com

ScienceDirect

Mendeleev Commun., 2024, **34**, 634–636

Mendeleev Communications

Luminescent properties and thermal stability of $(Lu_{0.98}Eu_{0.02})_2bdc_3{\cdot}10H_2O$ metal–organic frameworks

Yulia N. Toikka,*[a] Alexander R. Badikov,[a] Nikita A. Bogachev,[a] Ilya E. Kolesnikov,[a] Mikhail Yu. Skripkin,[a] Sergey N. Orlov[a,b] and Andrey S. Mereshchenko*[a]

[a] *Institute of Chemistry, St. Petersburg State University, 199034 St. Petersburg, Russian Federation. E-mail: y.toykka@spbu.ru, a.mereshchenko@spbu.ru*

[b] *Institute of Nuclear Industry, Peter the Great St. Petersburg Polytechnic University, 195251 St. Petersburg, Russian Federation*

DOI: 10.1016/j.mencom.2024.09.003

Two new heterometallic lutetium(III)–europium(III) terephthalate metal–organic frameworks were synthesized. The compounds demonstrated bright red emission of Eu^{3+} ions upon UV excitation into the $^1\pi\pi^*$ excited state of terephthalate anion. Photoluminescence properties of the compounds were shown to be determined by the local environment of europium ions.

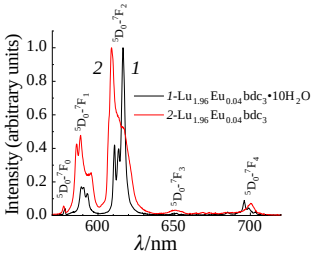

Keywords: europium, lutetium, metal–organic framework, photoluminescence, heterometallic, terephthalate.

Design of rare earth element-based materials with intensive luminescent properties is an actual and perspective area nowadays.[1–9] It is well-known that the direct photoexcitation of lanthanide ions is inefficient because 4f–4f transitions are forbidden. This obstacle can be overcome using the energy transfer from the excited ligand to the lanthanide ion, which is called the 'antenna effect'.[10,11] The aromatic organic entities such as 1,4-benzenedicarboxylate (terephthalate, bdc) are widely known as antenna ligands.[12,13] The enhancement of luminescence of metal–organic frameworks (MOFs) containing Eu^{3+} and Tb^{3+} upon doping with Gd^{3+} ions without crystalline phase change was reported previously.[14] Meanwhile, we demonstrated that lutetium doping of europium(III)[15] and terbium(III)[16] terephthalate MOFs significantly affects not only optical properties but also phase composition of such materials. However, it was not always possible to obtain one stable phase; instead, a mixture of phases was formed in heterometallic systems of lanthanide terephthalates, hampering the exploration of luminescent properties. In the current work we synthesized and established the composition and photophysical properties of new heterometallic lutetium(III)–europium(III) terephthalate MOFs containing a small amount of Eu^{3+} ions. Details of synthesis and analytical data are given in Online Supplementary Materials. MOF $(Lu_{0.98}Eu_{0.02})_2bdc_3{\cdot}10H_2O$ (**1**) was synthesized from aqueous solutions of lanthanide chlorides and sodium terephthalate. The PXRD data [Figure S1(*a*), Online Supplementary Materials] show that **1** is isostructural to $Lu_2bdc_3{\cdot}10H_2O$,[17] demonstrating that Eu^{3+} isomorphously substitutes Lu^{3+} ions in the crystal lattice. The Lu^{3+} ions in the $Lu_2bdc_3{\cdot}10H_2O$ structure are octacoordinated,[17] their coordination sphere consisting of four oxygen atoms from three bdc^{2-} ligands and four from water molecules (Figure S2, Online Supplementary Materials). According to the temperature-dependent PXRD in the 80–95 °C temperature range, compound **1** is dehydrated with the formation of compound **2** with an unknown amount of water. The PXRD pattern [Figure S1(*b*), Online Supplementary Materials] of compound **2** does not correspond to any of the known crystalline phases of anhydrous or low-water isomorphic lanthanide terephthalate.[18,19] The PXRD pattern of **2** consists of wide reflexes, indicating the poor crystallinity or very small crystallite size of **2**. To confirm the composition of **1** and to determine the number of water molecules per formula unit in **2**, TGA analysis was performed (Figure S3, Online Supplementary Materials). In the TGA curve, the weight loss of about 17.1% was observed, which corresponds to 10 water molecules per formula unit. Thus, substance **2** is an anhydrous compound $(Lu_{0.98}Eu_{0.02})_2bdc_3$. However, the PXRD pattern of **2** is different from the PXRD pattern of the typical crystalline anhydrous terephthalate, such as Ln_2bdc_3 (Ln = Tb, Eu, and Er).[18,20] Additional methods confirming the particular chemical composition of compounds **1** and **2** were elemental analysis, EDX and IR spectroscopy (Online Supplementary Materials). Therefore, it can be concluded that the new crystalline phase of anhydrous lanthanide(III) terephthalate (Ln_2bdc_3) was obtained.

We thoroughly explored the photophysical properties of MOFs **1** and **2**. Their emission spectra were measured upon 300 nm

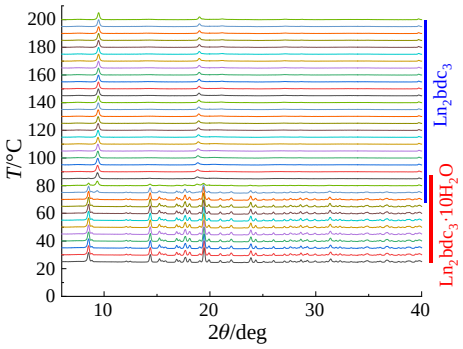

Figure 1 Temperature-dependent X-ray diffraction pattern for **1**.

excitation of the $^1\pi\pi$ terephthalate band [Figure 2(*a*)]. They consist of narrow bands corresponding to the $^5D_0$–^7F_J (J = 0–4) transitions of Eu^{3+}: $^5D_0$–$^7F_0$ (578.4 nm), $^5D_0$–$^7F_1$ (589, 590.6, and 593.2 nm), $^5D_0$–$^7F_2$ (610.8, 613.6, and 614.4 nm), $^5D_0$–$^7F_3$ (651.0 nm), and $^5D_0$$^7F_4$ (696, 699, and 703.6 nm), compound **1**; $^5D_0$–$^7F_0$ (577.4 nm), $^5D_0$–$^7F_1$ (586.0, 588.6, and 595.4 nm), $^5D_0$–$^7F_2$ (608.8 nm and a shoulder at 671 nm), $^5D_0$–$^7F_3$ (651.0 nm) and $^5D_0$–$^7F_4$ (700.6 nm), compound **2**. The $^5D_0$–$^7F_2$ bands are the most intense. The excitation spectra of **1** and **2** were measured at the emission maxima, 616 and 609 nm, respectively [Figure 2(*b*)]. Excitation spectra consist of broad bands corresponding to the transitions into $^1\pi\pi^*$ electronic excited states of the terephthalate ion:[15,21] 310 nm band with a 290 nm shoulder for compound **1** and 316 nm band with a 284 nm shoulder for compound **2**. Therefore, MOFs **1** and **2** demonstrate bright red emission corresponding to the $^5D_0$–^7F_J (J = 0–4) transitions of Eu^{3+} ions upon 300 nm excitation into the singlet electronic excited state of terephthalate ions due to the 'antenna' effect where the terephthalate ion as a synthesizer or 'antenna' effectively absorbs UV radiation and transfers energy to a luminescent lanthanide ion followed by the emission from lanthanide.[21] The fine structures of the $^5D_0$–^7F_J emission bands of **1** and **2** are different. The fine structure of the emission spectra depends on the crystalline phase due to the different local symmetry of the Eu^{3+} ions in different types of crystalline structures **1** and **2**. The analysis of the asymmetry ratio R_{21}, which is equal to the ratio of the integral intensity of ($^5D_0$–$^7F_2$) and ($^5D_0$–$^7F_1$) bands, allows one to track the changes in the local environment of the Eu^{3+} ions. The higher value of the asymmetry ratio R_{21} of **1** compared to that of **2** (Table 1) reflects the larger deviation from centrosymmetric environment of the Eu^{3+} in MOF **1**.[22–24] Photoluminescence decay curves of **1** and **2** were measured upon 300 nm excitation and monitored at the $^5D_0$–$^7F_2$ transition emission maxima, 616 and 609 nm, respectively [Figure 2(*c*)]. The decay curves were fitted by a sum of the two exponential functions, and then the average luminescence lifetime (τ_{av}), which corresponds to the $^5D_0$ level lifetime, was calculated (Online Supplementary Materials). Luminescence decay is affected by the combination of radiative and non-radiative processes. Decay rates and quantum efficiencies of the $^5D_0$ level of MOFs **1** and **2** are summarized in Table 1. We observed that the $^5D_0$ level lifetime τ_{av} of **1**, 0.245 ms, is significantly smaller than that of **2**, 1.842 ms. The water molecules in the $Ln_2bdc_3{\cdot}10H_2O$ structure are coordinated to the Eu^{3+} ion and quench Eu^{3+} luminescence due to the efficient energy transfer to high-energy O–H stretching vibrational modes.[25,26] In the Ln_2bdc_3 crystalline phase, the Eu^{3+} ion can be coordinated only to the oxygen atoms of terephthalate carboxylic groups.

The efficient quenching of Eu^{3+} ion luminescence by water molecules in the $Ln_2bdc_3{\cdot}10H_2O$ structure compared to the anhydrous Ln_2bdc_3 results in a significant decrease in the Eu^{3+} ion $^5D_0$ level lifetime as a result of the increase in the non-radiative rate A_{nr}. Furthermore, the quantum efficiency of the $^5D_0$ level of Eu^{3+} in **1** (6.6%) is significantly lower than that of **2** (30.6%) as a result of the luminescence quenching of electronically excited Eu^{3+} ions by water molecules in **1**. The photoluminescence quantum yield (PLQY, Table 1) of **1**, 6%, is twice as low than that of **2**, 13%. Interestingly, PLQY of **2**, $(Lu_{0.98}Eu_{0.02})_2bdc_3$, is lower than PLQY of $(Lu_{0.98}Eu_{0.02})_2bdc_3$ previously reported by our group (22%).[15] This observation can be explained by the difference in the crystalline phases of two anhydrous Eu–Lu terephthalates obtained in the current work and in the previous one.[15] Therefore, $(Lu_{0.98}Eu_{0.02})_2bdc_3$[15] is isostructural to Tb_2bdc_3,[18] whereas $(Lu_{0.98}Eu_{0.02})_2bdc_3$ obtained in this work using a slightly different synthesis procedure has the same composition, but different crystalline structure. Two main factors that determine the value of the PLQY of Eu^{3+}-based antenna MOFs are: (i) the efficiency of the energy transfer between the organic ligand sensitizer and the europium ion and (ii) the quantum efficiency of the $^5D_0$ level of Eu^{3+} mainly affected by the non-radiative processes resulting in emission quenching. To estimate the efficiency of the energy transfer from the terephthalate ion to Eu^{3+}, we calculated the quantum yield of $^5D_0$ level formation as $\Phi_{form}(^5D_0)$ = PLQY/$\phi(^5D_0)$, Table 1. We have found that the quantum yield of the formation of the $^5D_0$ level of **1**, 92%, is twice as high than that of **2**, 42%. Therefore, the energy transfer is less efficient in anhydrous Eu–Lu terephthalate **2** than in decahydrate **1**, which is probably caused by the more pronounced π-stacking in the crystalline structure of **2** compared to **1**. Meanwhile, the luminescence quenching of electronically excited Eu^{3+} ions by water molecules dominates over the energy transfer effect. As a result, the PLQY of **2** is larger than that of **1**.

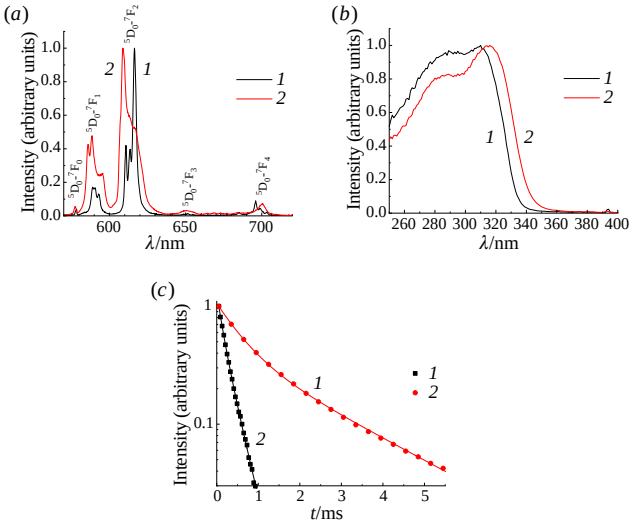

Figure 2 (*a*) Emission spectra of MOFs **1** and **2** upon 300 nm excitation; (*b*) excitation spectra of MOFs **1** and **2** measured at the emission wavelength of 616 and 609 nm, respectively; and (*c*) the photoluminescence decay curves of MOFs **1** and **2** upon 300 nm excitation at the emission wavelength of 616 and 609 nm, respectively.

In summary, two new heterometallic lutetium(III)–europium(III) terephthalate MOFs $(Lu_{0.98}Eu_{0.02})_2bdc_3{\cdot}10H_2O$ (**1**) and $(Lu_{0.98}Eu_{0.02})_2bdc_3$ (**2**) were obtained. Furthermore, we have discovered the new crystalline modification of anhydrous lanthanide terephthalate, which is represented by MOF **2**. The both MOFs demonstrate bright red emission of Eu^{3+} ions upon UV excitation into $^1\pi\pi^*$ states of terephthalate ions due to the

Table 1 Photophysical properties of MOFs **1** and **2**.[a]

Sample	τ_1/ms	τ_2/ms	τ_{av}/ms	A_{tot}/s^{-1}	A_r/s^{-1}	A_{nr}/s^{-1}	$\phi(^5D_0)$ (%)	PLQY (%)	$\Phi_{form}(^5D_0)$ (%)	R_{21}
1	0.14 ± 0.02 (45%)	0.29 ± 0.02 (55%)	0.245	4040	264	3776	6.5	6 ± 1	92	3.81
2	0.59 ± 0.02 (60%)	2.32 ± 0.07 (40%)	1.842	543	166	377	30.6	13 ± 1	42	2.14

[a] τ_1 and τ_2 are the photoluminescence decay time constants (the fractions of the exponential components are given in parentheses); τ_{av} is the $^5D_0$ level lifetime; A_r, A_{nr}, and A_{tot} are the radiative, non-radiative, and total decay rates, respectively; $\phi(^5D_0)$ and $\Phi_{form}(^5D_0)$ are the quantum efficiencies and formation quantum yields of the $^5D_0$ level; PLQY is the photoluminescence quantum yield; and R_{21} is the asymmetric ratio. The methodology for measuring the above-mentioned physical quantities is given in Online Supplementary Materials.

'antenna' effect. The lifetime of the Eu^{3+} $^5D_0$ level and the quantum efficiency of **1** is significantly smaller than that of **2** because the water molecules in **1** increase the probability of non-radiative transitions due to efficient energy transfer to high-energy O–H stretching modes. The photoluminescence quantum yield of **2** is larger than that of **1**. The antenna effect is less pronounced in anhydrous Eu–Lu terephthalate **2** than in decahydrate **1**.

The measurements were performed in the Research Park of Saint-Petersburg State University (Magnetic Resonance Research Centre, Chemical Analysis and Materials Research Centre, Cryogenic Department, Interdisciplinary Resource Centre for Nanotechnology, Centre for X-ray Diffraction Studies, Centre for Optical and Laser Materials Research, Thermogravimetric and Calorimetric Research Centre, and Centre for Innovative Technologies of Composite Nanomaterials). This work was supported by the Russian Science Foundation (grant no. 22-73-10040, https://rscf.ru/en/project/22-73-10040/, accessed on 16.04.2024). The authors thank Maxim Bezrukaviy and Anastasiya Nikolaeva for the contribution to the experimental part of the work.

Online Supplementary Materials

Supplementary data associated with this article can be found in the online version at doi: 10.1016/j.mencom.2024.09.003.

References

1 A. V. Shurygin, V. I. Vovna, V. V. Korochentsev, A. G. Mirochnik, I. V. Kalinovskaya and V. I. Sergienko, *Spectrochim. Acta, Part A*, 2021, **250**, 119397; https://doi.org/10.1016/j.saa.2020.119397.
2 M. I. Kozlov, A. N. Aslandukov, A. A. Vashchenko, A. V. Medvedko, A. E. Aleksandrov, R. Grzibovskis, A. S. Goloveshkin, L. S. Lepnev, A. R. Tameev, A. Vembris and V. V. Utochnikova, *Dalton Trans.*, 2019, **48**, 17298; https://doi.org/10.1039/C9DT03823J.
3 X. Zhou, H. Wang, S. Jiang, G. Xiang, X. Tang, X. Luo, L. Li and X. Zhou, *Inorg. Chem.*, 2019, **58**, 3780; https://doi.org/10.1021/acs.inorgchem.8b03319.
4 D. Liu, K. Lu, C. Poon and W. Lin, *Inorg. Chem.*, 2014, **53**, 1916; https://doi.org/10.1021/ic402194c.
5 V. Khudoleeva, L. Tcelykh, A. Kovalenko, A. Kalyakina, A. Goloveshkin, L. Lepnev and V. Utochnikova, *J. Lumin.*, 2018, **201**, 500; https://doi.org/10.1016/j.jlumin.2018.05.002.
6 D. A. Bardonov, L. N. Puntus, I. V. Taidakov, E. A. Varaksina, K. A. Lyssenko, I. E. Nifant'ev and D. M. Roitershtein, *Mendeleev Commun.*, 2022, **32**, 198; https://doi.org/10.1016/j.mencom.2022.03.015.
7 A. A. Botnar, T. V. Tikhomirova and A. S. Vashurin, *Mendeleev Commun.*, 2023, **33**, 729; https://doi.org/10.1016/j.mencom.2023.09.044.
8 L. N. Puntus, D. A. Bardonov, E. A. Varaksina, I. V. Taydakov, D. M. Roitershtein, I. E. Nifant'ev and K. A. Lyssenko, *Mendeleev Commun.*, 2024, **34**, 325; https://doi.org/10.1016/j.mencom.2024.04.005.
9 V. K. Brel, A. V. Vologzhanina, M. T. Metlin and I. V. Taydakov, *Mendeleev Commun.*, 2024, **34**, 329; https://doi.org/10.1016/j.mencom.2024.04.006.
10 H.-Q. Yin, X.-Y. Wang and X.-B. Yin, *J. Am. Chem. Soc.*, 2019, **141**, 15166; https://doi.org/10.1021/jacs.9b06755.
11 W. Cao, Y. Tang, Y. Cui and G. Qian, *Small Struct.*, 2020, **1**, 2000019. DOI: 10.1002/sstr.202000019.
12 J. F. S. do Nascimento, B. S. Barros, J. Kulesza, J. B. L. de Oliveira, A. K. P. Leite and R. S. de Oliveira, *Mater. Chem. Phys.*, 2017, **190**, 166; https://doi.org/10.1016/j.matchemphys.2017.01.024.
13 S. S. Kolesnik, V. G. Nosov, I. E. Kolesnikov, E. M. Khairullina, I. I. Tumkin, A. A. Vidyakina, A. A. Sysoeva, M. N. Ryazantsev, M. S. Panov, V. D. Khripun, N. A. Bogachev, M. Yu. Skripkin and A. S. Mereshchenko, *Nanomaterials*, 2021, **11**, 2448; https://doi.org/10.3390/nano11092448.
14 V. V. Utochnikova and N. P. Kuzmina, *Russ. J. Coord. Chem.*, 2016, **42**, 679; https://doi.org/10.1134/S1070328416090074.
15 V. G. Nosov, A. S. Kupryakov, I. E. Kolesnikov, A. A. Vidyakina, I. I. Tumkin, S. S. Kolesnik, M. N. Ryazantsev, N. A. Bogachev, M. Yu. Skripkin and A. S. Mereshchenko, *Molecules*, 2022, **27**, 5763; https://doi.org/10.3390/molecules27185763.
16 V. G. Nosov, Y. N. Toikka, A. S. Petrova, O. S. Butorlin, I. E. Kolesnikov, S. N. Orlov, M. N. Ryazantsev, S. S. Kolesnik, N. A. Bogachev, M. Yu. Skripkin and A. S. Mereshchenko, *Molecules*, 2023, **28**, 2378; https://doi.org/10.3390/molecules28052378.
17 P. Wang, Z.-F. Li, L.-P. Song, C.-X. Wang and Y. Chen, *Acta Crystallogr., Sect. E: Struct. Rep. Online*, 2006, **62**, m253; https://doi.org/10.1107/S1600536806000225.
18 T. M. Reineke, M. Eddaoudi, M. Fehr, D. Kelley and O. M. Yaghi, *J. Am. Chem. Soc.*, 1999, **121**, 1651; https://doi.org/10.1021/ja983577d.
19 R. A. Zehnder, R. A. Renn, E. Pippin, M. Zeller, K. A. Wheeler, J. A. Carr, N. Fontaine and N. C. McMullen, *J. Mol. Struct.*, 2011, **985**, 109; https://doi.org/10.1016/j.molstruc.2010.10.030.
20 C. Daiguebonne, N. Kerbellec, O. Guillou, J.-C. Bünzli, F. Gumy, L. Catala, T. Mallah, N. Audebrand, Y. Gérault, K. Bernot and G. Calvez, *Inorg. Chem.*, 2008, **47**, 3700; https://doi.org/10.1021/ic702325m.
21 V. V. Utochnikova, A. Yu. Grishko, D. S. Koshelev, A. A. Averin, L. S. Lepnev and N. P. Kuzmina, *Opt. Mater. (Amsterdam, Neth.)*, 2017, **74**, 201; https://doi.org/10.1016/j.optmat.2017.02.052.
22 E. V. Golyeva, I. E. Kolesnikov, E. Lähderanta, A. V. Kurochkin and M. D. Mikhailov, *J. Lumin.*, 2018, **194**, 387; https://doi.org/10.1016/j.jlumin.2017.10.068.
23 K. Park, H. Kim and D. A. Hakeem, *Dyes Pigm.*, 2017, **136**, 70; https://doi.org/10.1016/j.dyepig.2016.08.022.
24 E. W. J. L. Oomen and A. M. A. van Dongen, *J. Non-Cryst. Solids*, 1989, **111**, 205; https://doi.org/10.1016/0022-3093(89)90282-2.
25 M. Li, Y. Zhou, Y. Yao, T. Gao, P. Yan and H. Li, *Dalton Trans.*, 2021, **50**, 9914; https://doi.org/10.1039/D1DT00155H.
26 A. A. Ivanova, V. E. Gontcharenko, A. M. Lunev, A. V. Sidoruk, I. A. Arkhipov, I. V. Taydakov and Y. A. Belousov, *Inorganics*, 2022, **10**, 104; https://doi.org/10.3390/inorganics10080104.

Received: 21st May 2024; Com. 24/7499